Time-matched pre- and postsynaptic changes of GABAergic synaptic transmission in the developing mouse superior colliculus

Sergei Kirischuk[1], René Jüttner[2] and Rosemarie Grantyn[1]

[1]*Developmental Physiology, Johannes Müller Institute of Physiology, Humboldt University Medical School (Charité), 10117 Berlin, Germany*
[2]*Developmental Neurobiology, Max-Delbrück Center, 13092 Berlin-Buch, Germany*

Developmental changes in the kinetics of GABAergic postsynaptic currents have been reported for various brain structures. However, it has remained unclear whether these modifications are matched by presynaptic changes. We addressed this question by analysing evoked IPSCs (eIPSCs) in mouse superior colliculus slices between postnatal day (P) 1 and 22. eIPSCs were elicited by electrical stimulation and measured in the whole-cell patch-clamp configuration. IPSCs were analysed using the binomial model of synaptic transmission. The readily releasable pool (RRP, N) was estimated from the cumulative eIPSC amplitude histograms during 50-Hz stimulation. Median delayed IPSC (dIPSC) amplitude was used as a quantal amplitude (q) estimate. The mean release probability (p) was determined as the mean eIPSC amplitude divided by the product of RRP and q. The experiments revealed that GABAergic synapses pass through two distinct periods of functional adjustment: (i) P1–3 (coincidental with the onset of glutamatergic spontaneous activity and a switch from depolarizing to hyperpolarizing GABA action) displayed a significant decrease of p, associated with an increase in the paired-pulse ratio ($eIPSC_2/eIPSC_1$); and (ii) P6–15 (the period before and shortly after eye opening) is characterized by a drastic reduction of IPSC duration. On the presynaptic side, it was accompanied by a down-regulation of asynchronous release in favour of stimulus-locked synchronous release. We conclude that postsynaptic modifications of GABAergic synaptic transmission in the superior colliculus (SC) are indeed accompanied by presynaptic changes, and this may guarantee the necessary efficacy of inhibition during the developmental reconstruction of the synaptic network in the SC.

(Resubmitted 13 December 2004; accepted after revision 19 January 2005; first published online 20 January 2005)
Corresponding author S. Kirischuk: Developmental Physiology, Johannes Müller Institute of Physiology, Humboldt University Medical School (Charité), 10117 Berlin, Germany. Email: sergei.kirischuk@charite.de

Synaptic transmission is subject to permanent adjustment. During development, individual contacts undergo marked changes that contribute to the fine-tuning of the network performance in response to variable functional demands. On the other hand, reliable information transfer requires an exact match between presynaptic and postsynaptic sites despite the necessary developmental re-organization. On the postsynaptic side, the subunit composition of postsynaptic receptors is altered which affects the kinetics of postsynaptic responses (Mishina *et al.* 1986; Fritschy *et al.* 1994; Okada *et al.* 2000; Juttner *et al.* 2001; Iwasaki & Takahashi, 2001). On the presynaptic side, the previously reported developmental changes include: (i) shortening of presynaptic action potentials (Taschenberger & von Gersdorff, 2000); (ii) modifications in the presynaptic Ca^{2+} channel spectrum (Iwasaki *et al.* 2000); and (iii) lowering of release probability along with a switch from paired-pulse depression to paired-pulse facilitation (Pouzat & Hestrin, 1997; Iwasaki & Takahashi, 2001), attenuation of tetanic synaptic depression during stimulus trains (Taschenberger & von Gersdorff, 2000; Brenowitz & Trussell, 2001) and a decrease in the mean quantal content (Bolshakov & Siegelbaum, 1995; Pouzat & Hestrin, 1997). However, most of these changes were observed in experiments with excitatory glutamatergic synapses (Taschenberger & von Gersdorff, 2000; Chuhma *et al.* 2001; Brenowitz & Trussell, 2001; Mori-Kawakami *et al.* 2003). The development of inhibitory synaptic transmission in the brain has received much less attention (but see Pouzat & Hestrin, 1997; Gubellini *et al.* 2001).

S. Kirischuk and R. Jüttner contributed equally to this work.

DOI: 10.1113/jphysiol.2004.081216

We chose to study the development of inhibitory synaptic transmission in the superficial layers of the mouse superior colliculus (SC), a structure that is reputed to contain the highest concentration of GABA in the CNS and a very high density of GABAergic synaptic terminals (for review see Mize, 1996; Grantyn *et al.* 2004). In the rodent SC, GABAergic synapses already exist before birth (Meier *et al.* 2003). Until P2, GABA release induces depolarization and Ca^{2+} elevation, but from P3 onwards GABA acts as inhibitory neurotransmitter (Grantyn *et al.* 2004). During the period P6–8, the cortico-tectal pathway is being formed and is then ready to contribute to excitatory synaptic activity in the SC (Thong & Dreher, 1986). By P15, i.e. after eye opening, synaptogenesis in the SC reaches a peak (Warton & McCart, 1989), followed by a period when synapse pruning outbalances the development of new synapses. By P22, GABAergic synapses display mature characteristics; that is, they generate stimulus-locked short IPSCs and preferentially display paired-pulse facilitation (Juttner *et al.* 2001). Thus, between P1 and P22 GABAergic synapses formed by intrinsic GABAergic interneurones in the SC must be adjusted to two major waves of glutamatergic up-regulation: (i) (P1–3) due to the maturation of the retino-tectal pathway; and (ii) (P6–P15) associated with the maturation of the cortico-tectal input. In its turn, GABAergic synaptic transmission is supposed to play an important role in the formation and re-modelling of visual maps in the SC (Zhang *et al.* 1998; Holt & Harris, 1998).

We have recently reported that maturation of GABAergic synaptic transmission in the SC implies an age-dependent shortening of IPSCs and a switch from paired-pulse depression to paired-pulse facilitation (Juttner *et al.* 2001). However, our previous report was confined to comparison of GABAergic synaptic transmission at two developmental stages, the early postnatal period immediately after birth (P1–3) and maturity (P20–22). Therefore the precise timing of pre- and postsynaptic parameters has remained unexplored. In the present work, experiments were performed at a finer time scale including six age groups from P1 to P22. This allowed us to address the following two main questions. (i) Do presynaptic changes in GABA release occur in synchrony with changes of postsynaptic $GABA_A$ receptor function? (ii) Are these changes continuous or confined to distinct periods in the development of the SC, such as the onset of retino-tectal or cortico-tectal activity?

Methods

Slice preparation

All experiments were conducted with pigmented mice (C57BL/6J) pups between postnatal day (P) 1 and 22 (the day of birth was taken as P0). Collicular slices were prepared as previously described (Juttner *et al.* 2001). Briefly, animals were decapitated under halothane anaesthesia. The brain was removed quickly and transferred into an ice-cold artificial cerebrospinal fluid (ACSF). Horizontal slices (150 μm thick) of the SC were prepared by vibratome (Integraslice 7550PSDS, Campden Instruments Ltd, Loughborough, UK). Before testing, slices were stored for at least 1 h at room temperature (23–25°C) in standard ACSF containing (mM): NaCl 125, KCl 5, $MgCl_2$ 1, $CaCl_2$ 2, NaH_2PO_4 1.25, $NaHCO_3$ 25 and glucose 5; pH was buffered to 7.3 by continuous bubbling with 5% CO_2–95% O_2. All experiments were carried out according to the guidelines laid down by the Office for Health Protection and Technical Safety of the Regional Government, Berlin (T0406/98).

Electrophysiological recordings

For electrophysiological recordings, slices were transferred into a submersion chamber on the microscope stage (Axioscope FS, Zeiss, Oberkochen, Germany) and continuously superfused (1 ml min^{-1}) with oxygenated ACSF. A 63× water immersion objective (Zeiss) was used in all experiments. Differential interference contrast optics were applied to visualize cells. The whole-cell patch-clamp technique was applied to record inhibitory postsynaptic currents (IPSCs). The pipette solution contained (mM): potassium gluconate 100, KCl 50, NaCl 5, $MgCl_2$ 2, $CaCl_2$ 1, EGTA 10 and Hepes 20; the pH was set to 7.2 with KOH. N-(2,6-dimethylphenylcarbamoylmethyl)-triethylammonium bromide (QX 314, 2 mM) was added to the intrapipette solution to prevent generation of action potentials in the tested neurones. Lucifer Yellow (0.1 mg ml^{-1}, Sigma) was always added to the pipette solution to visualize the investigated cells. The series resistance was less than 15 MΩ and was partially compensated (50–70%). Before stimulation, the access resistance was always controlled by applying hyperpolarizing pulses of 10 mV. Cells exhibiting more than 10% changes in the access resistance were discarded. Recordings were carried out using an EPC-7 amplifier (List, Darmstadt, Germany). Signals were filtered at 3 kHz and sampled at a rate of 10 kHz and analysed off-line using the software TIDA 4.11 (HEKA Electronics, Lambrecht/Pfalz, Germany). The chloride reversal potential was about −20 mV. The holding potential was set to −70 mV.

GABAergic IPSCs were isolated pharmacologically. The AMPA receptor antagonist, 6,7-dinitroquinoxaline-2,3-dione (DNQX, 20 μM), the NMDA receptor blocker, DL-2-amino-5-phosphonopentanoic acid (APV, 100 μM), the glycine receptor antagonist, strychnine (0.5 μM) and the nicotinic acetylcholine receptor

blocker, D-tubocurarine (5 μM) were added to the ACSF.

Cell selection and electrical stimulation

The criteria for neurone selection were described elsewhere (Juttner *et al.* 2001). Briefly, neurones were qualified according to the size of their soma and according to the extension of their dendritic tree, after filling them with Lucifer Yellow. At P1–3 neurones with a soma diameter of $< 12\,\mu$m and less than three stem dendrites were rejected. In older preparations it was also required that the dendritic field projection exceeded 200 μm in diameter. Based on these criteria it is very likely that recordings were performed on the class described as 'wide field neurones' (Grantyn *et al.* 2004).

Postsynaptic currents were elicited by focal electrical stimulation through glass pipettes filled with the ACSF (1–3 MΩ) and placed within the limits of the dendritic tree. An isolated stimulation unit was used to generate rectangular electrical pulses (0.5 ms) at a frequency of 1 s^{-1}. The intensity of test pulses was varied between 1 and 4 μA. In the lower intensity range, IPSC amplitudes increased with stimulus intensity, presumably through recruitment of presynaptic cells/axons. After the saturating intensity was reached, the average IPSC amplitudes were no longer dependent on the stimulus strength which presumably reflects an activation of all presynaptic elements located in the vicinity of the stimulation pipette. To perform the protocols described in the results, a supra-maximal intensity (i.e. the stimulus strength was 1.3–1.5 times larger than the saturating intensity of 1.5–2 μA) was used. The pulse duration was set to 0.5 ms.

The following stimulation protocol was applied in this study. At the beginning of each experiment, 10 single eIPSCs were recorded from the neurone of interest. The stimulation frequency was 0.2 Hz. Next, trains of pulses were applied. The stimulation frequency was always 50 Hz. The number of pulses in the trains was variable (two to 80 stimuli). Each stimulus train was repeated at least 10 times. The period between successive trains was 1 min. Figure 1*A* shows individual postsynaptic responses induced by a single stimulus and a train of 20 pulses at 50 Hz. The mean amplitude of the first eIPSC in the trains was used to control the stability of synaptic activation. Neurones exhibiting a more than 20% change in the eIPSC amplitude were discarded.

Analysis of postsynaptic responses

The present work relies on the assumption that IPSCs could well be approximated by the binomial model of synaptic transmission (del Castillo & Katz, 1954). This model suggests that: (i) there are a constant number of release sites (N) which liberate vesicles with an average probability of p; (ii) a single vesicle produces an invariant (quantal) IPSC (q); (iii) all release sites are independent;

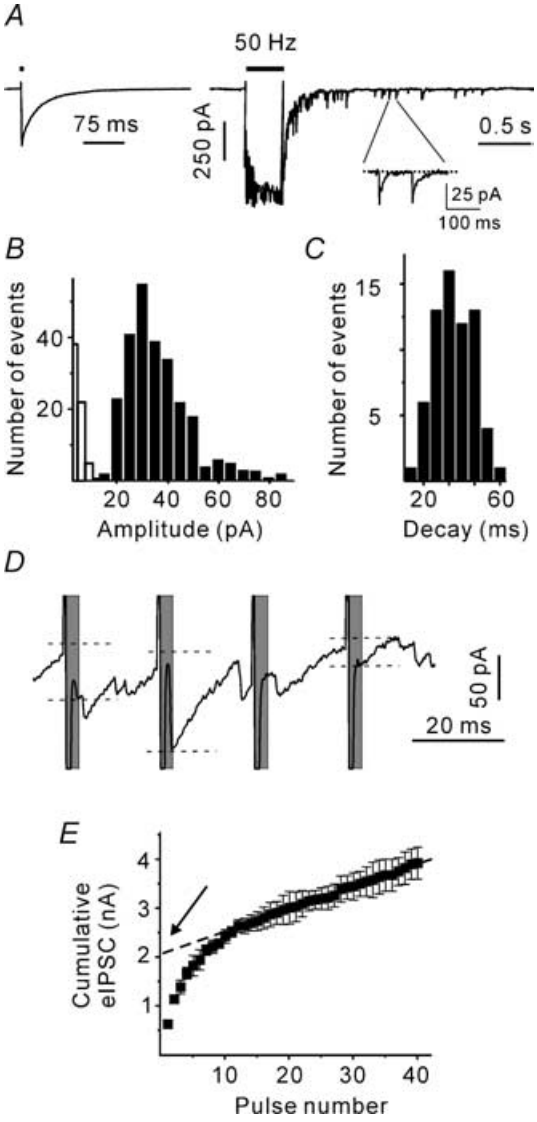

Figure 1. Estimation of synaptic transmission parameters
A, sample trace representing a single eIPSC and a compound postsynaptic response induced by a train of 20 pulses delivered at 50 Hz (mouse at P1). Stimulation artefacts were partially blanked for clarity. The inset shows delayed IPSCs (dIPSCs) selected for the calculation of the dIPSC decay time constant. *B*, dIPSC amplitude histogram. Open columns show the noise distribution. *C*, distribution of dIPSC decay time constants. *D*, eIPSCs during the late phase of stimulation protocol. Only events that occurred within a 3-ms interval after the stimulus termination (shaded areas) were selected as eIPCSs. To measure the eIPSC amplitudes (shown by dashed lines), a linear fit of the decay of the preceding IPSC was first subtracted from each event. *E*, cumulative eIPSC amplitude during a 50 Hz train. The dotted line represents a linear fit to the last 20 stimuli during the train back-extrapolated to time 0. The *y* intersect gives an estimate of the RRP in the absence of pool replenishment.

and (iv) each release site liberates either a single vesicle or nothing in response to an action potential. In the frame of the binomial model, the mean eIPSC amplitude is given by:

$$\text{eIPSC} = Npq \quad (1)$$

The quantal parameters (q, N, p) were obtained as follows. Repetitive stimulation causes a compound postsynaptic response (Fig. 1*A*). IPSCs that were generated after the termination of stimulation are referred to as delayed IPSCs (dIPSCs). As tetrodotoxin was not added to the ASCF, dIPSCs represent spontaneous IPSCs. Delayed IPSCs were used to estimate the quantal size (q). Delayed IPSCs were recorded within the first 3 s after the termination of stimulation. As spontaneous IPSC frequency was lower than 2 Hz at all ages studied (Juttner *et al.* 2001), a possible contribution of spontaneous IPSCs originating from non-stimulated synaptic contacts was ignored. The dIPSC distribution was skewed (Fig. 1*B*). This is the reason why we used the median dIPSC amplitude rather than the arithmetic mean as an estimate of q. In addition, rise times and time constants of decay (a single exponential fit) of individual dIPSCs were estimated (Fig. 1*C*). For each neurone, the mean rise time, the mean time constant of decay and the median dIPSC amplitude were used as a template to calculate the mean dIPSC charge transfer (q_c).

The number of release sites is difficult to measure directly. Therefore, the size of the readily releasable pool (RRP) has been frequently used as its approximate (Schneggenburger *et al.* 1999; Lu & Trussell, 2000; Kirischuk & Grantyn, 2003). To apply this method, one has to measure the amplitudes of stimulus-locked IPSCs. However, high frequency stimulation strongly increases the frequency of asynchronous events. To discriminate between stimulus-locked and asynchronous IPSCs, IPSCs that peaked within a 3-ms interval after the end of a stimulus pulse will be referred to as stimulus-locked eIPSCs. To measure the eIPSC amplitudes, a linear fit of the decay of the preceding IPSC was first subtracted from each event (Fig. 1*D*).

Repetitive stimulation leads to a decrease in the eIPSC amplitudes. Assuming that eIPSC depression is largely caused by a transient decrease in the number of readily releasable quanta, it is possible to estimate the RRP on the basis of cumulative eIPSC amplitudes. Cumulative eIPSC amplitudes were plotted *versus* stimulus number. After 10 pulses, the cumulative eIPSCs reached a steady state, as indicated by the linear slope dependency of the cumulative eIPSC amplitude on the pulse number (Fig. 1*E*). Assuming that (i) the number of release sites remains constant throughout the experiment and (ii) the linear component reflects vesicle recycling, the cumulative IPSC amplitude in the absence of pool replenishment can be estimated by back-extrapolation to the start of the train (Fig. 1*E*). Normalizing the obtained value to the median dIPSC amplitude provides an estimate for the RRP size.

Finally, eqn (1) was use to calculate the mean release probability (p):

$$p = \text{eIPSC}/(Nq) = \text{eIPSC}/(\text{RRP} \times \text{dIPSC}) \quad (2)$$

Calculation of eIPSC-mediated charge transfer during high frequency trains

Evoked IPSCs occurring during the stimulus train are supposed to exhibit a monoexponential decay with a time constant similar to that of single eIPSCs (τ). The rise time was neglected. Individual eIPSCs were modelled using the following function:

$$\text{eIPSC}(t) = \text{eIPSC}_{\text{amp}} \times \exp(-(t - t_0)/\tau), \qquad \text{if } t > t_0$$

$$\text{eIPSC}(t) = 0, \qquad \text{if } t < t_0$$

where t_0 is the time of occurrence and $\text{eIPSC}_{\text{amp}}$ is the eIPSC amplitude. The total eIPSC response elicited by high frequency stimulation was constructed as follows:

$$\text{eIPSC}(t) = \Sigma\text{eIPSC}_i \times \exp(-(t - i \times \text{ISI})/\tau) \quad (3)$$

where i is a pulse number (from 1 to 40), eIPSC_i is the measured stimulus-locked eIPSC amplitude, ISI is the interstimulus interval (20 ms in our case) and τ is the eIPSC decay time constant. The time origin is given by the first stimulus. The modelled eIPSC response was integrated (Microsoft Excel 2000) to obtain the synchronous charge transfer per stimulus. To minimize (i) the distortion of synaptic currents by stimulation artefacts, and (ii) the impact of neglected eIPSC rising phase on the calculated charge transfer, the first 3 ms after a stimulus were skipped and interstimulus integrals were calculated over 17-ms periods.

Superfusion

All experiments were performed at room temperature (23–25°C). A gravity-driven superfusion system was used. DNQX was obtained from Tocris (Bristol, UK). All other chemicals were purchased from Sigma-Aldrich (Taufkirchen, Germany).

Data analysis and statistics

IPSCs were analysed using the software PeakCount V3.2 (C. Henneberger, Berlin, Germany). The software employs a derivative threshold-crossing algorithm to detect IPSCs. Each automatically detected event was displayed for visual inspection. Rise times and time constants of decay (a single exponential fit) of individual IPSCs were calculated. When events overlapped, their decays were obscured

and therefore the kinetics of respective IPSCs were not analysed. To measure amplitudes, a linear fit of the decay of the preceding IPSC was first subtracted from each event. All results are presented as means ± S.E.M. with n indicating the number of cells tested. The error bars in all figures indicate S.E.M. All comparisons between means were tested for significance using the ANOVA test and Student's t test, unless otherwise stated. The symbols $*$ and $**$ denote significance levels of $P < 0.05$ and $P < 0.01$, respectively.

Results

Changes in the IPSC kinetics

Our group has recently reported that in mouse SC slices individual IPSCs recorded shortly after birth (P1–3) are significantly longer than the IPSCs recorded at P22 (Juttner *et al.* 2001). To investigate the developmental time course of IPSC shortening, we analysed the eIPSC decay time constants at different ages (Fig. 2*A*). Figure 2*B* shows that the eIPSC decay became faster with age. This change occurred between P6 and P15. The time constants of decay were 36 ± 3, 28 ± 2 and 22 ± 2 ms at P6 ($n = 9$), P11 ($n = 8$) and P15 ($n = 9$), respectively. The differences between these age groups were significant ($P < 0.05$; note that numbers of cells tested shown on the columns are valid for all following figures, except Fig. 8*B*).

The slower decay kinetics of immature synapses may be explained either by changes in the postsynaptic receptor composition (Juttner *et al.* 2001) or by a larger jitter in the GABA release. To examine the latter possibility we compared the decay kinetics of quantal events (dIPSCs) and eIPSCs. It was found that the dIPSC decay kinetics exhibited a similar change with age (Fig. 2*C*).

The maturation of synaptic contacts was reported to be accompanied by a decrease in the release probability (Bolshakov & Siegelbaum, 1995). Higher release probability at immature synapses may result in multiquantal release. This would lead to a higher concentration and longer presence of the transmitter in the synaptic cleft and could then account for the longer decay time constants of postsynaptic currents (Jones & Westbrook, 1995). If this were the case, the eIPSC decay kinetics would be expected to be longer than that of the supposedly mono-quantal dIPSCs. However, eIPSC and dIPSC decay time constants displayed a strong linear correlation at all ages tested. Figure 2*D* shows this relationship for P1 and P22. The slope of the linear fitting curve was not significantly different from one (minimal $P > 0.3$, one population Student's t test). We therefore conclude that the observed IPSC shortening has a postsynaptic origin.

Developmental decrease in the eIPSC amplitude is accompanied by changes in the number of release sites and release probability, but not dIPSC amplitude

Next we asked whether the eIPSC amplitudes change during development. Figure 3*A* shows that the mean eIPSC amplitude was, indeed, significantly larger at P1 than at older ages. Surprisingly, a strong decrease was observed already at P3 (268 ± 58 *versus* 505 ± 74 pA at P1, $P < 0.05$). To identify the factors underlying the observed

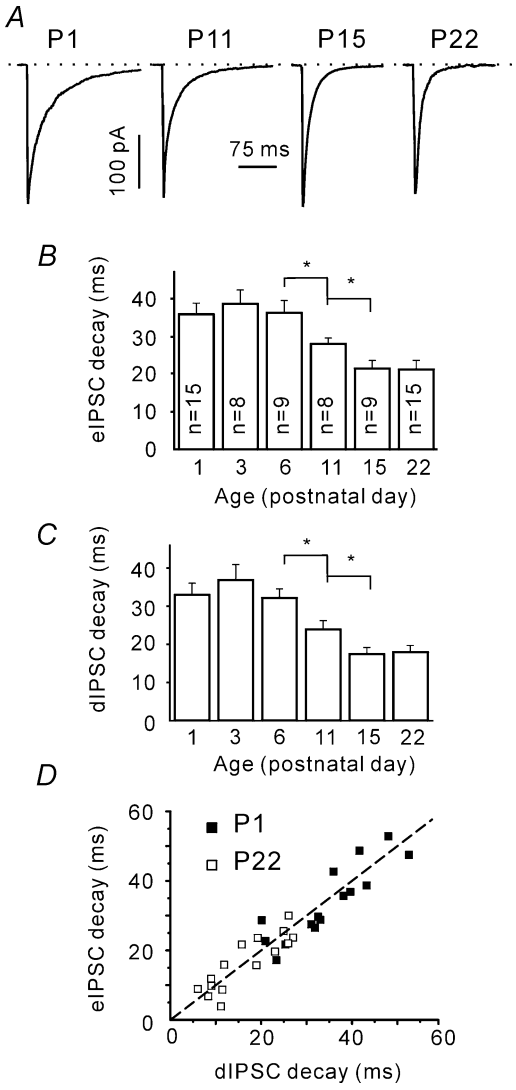

Figure 2. Age-dependent shortening of both eIPSCs and dIPSCs
A, sample traces represent eIPSCs recorded in slices prepared from mice of different ages. Each trace is an average of 10 single trials. *B*, age dependence of eIPSC decay time constants. Decay time constants were calculated using a single exponential fit. Numbers on columns indicate the number of cells tested and are valid for all following figures, except Fig. 8*B*. *C*, age dependence of dIPSC decay time constants. Note that both eIPSC and dIPSC decays exhibit an acceleration between P6 and P15. *D*, eIPSC and dIPSC decay time constants exhibit a strong linear correlation. The dashed line corresponds to a 1 : 1 ratio.

eIPSC amplitude changes, the binomial model of synaptic transmission was applied. In the frame of the binomial model, mean eIPSC amplitudes (i.e. the quantal content) represent the product of the number of release sites (N), the mean release probability (p) and the quantal amplitude (q).

First, we inspected whether q alters during early postnatal development. The median dIPSC amplitude was taken as an estimate for q (see Methods, Fig. 1*B*). Figure 3*B* shows that q did not display any age dependence. We therefore conclude that the developmental changes in the eIPSC amplitude were not due to a change in the quantal amplitude.

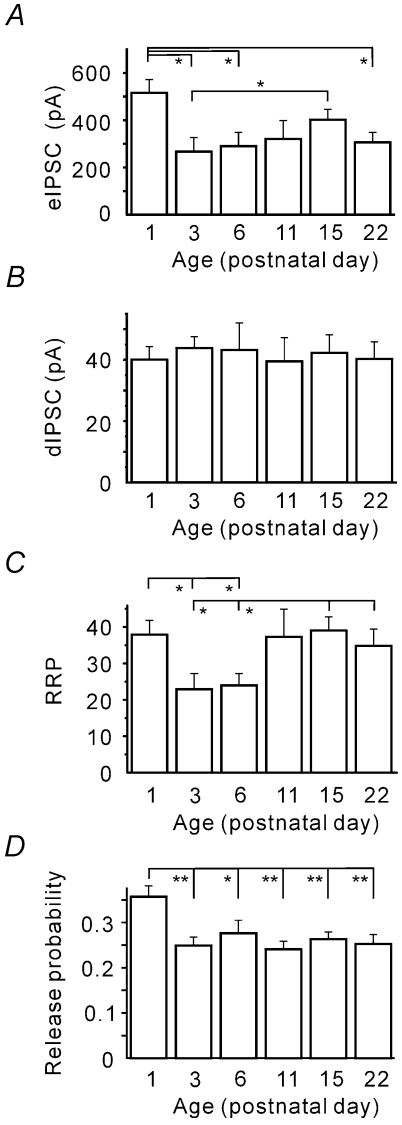

Figure 3. Developmental reduction of the quantal content (mean eIPSC amplitude) due to changes in the number of release sites and release probability
A, mean eIPSC amplitudes at different ages. *B*, the quantal size (median dIPSC amplitude) does not exhibit age dependence. *C*, RRP size is significantly smaller at P3 and P6. *D*, mean release probabilities (p = eIPSC/(RRP × dIPSC)) obtained for different ages. Note that a significant reduction in p occurred by P3.

Next we asked whether the number of release sites displayed a change with age. Figure 3*C* shows that the RRP size (see Methods, Fig. 1*E*) was significantly smaller in the P3 and P6 age groups (23 ± 4 and 24 ± 3, respectively) than at P1, P11, P15 and P22 (38 ± 4, 37 ± 7, 39 ± 4 and 35 ± 4, respectively, $P < 0.05$). However it is worth mentioning that the decrease in the RRP size observed at P3 and P6 could result from a decrease in either the number of synaptic contacts, or the number of synaptic connections, or both. Unfortunately, the method applied does not allow us to distinguish between these possibilities, and the physiological meaning of this observation needs further investigation.

Nevertheless, obtained estimates for the quantal size (median dIPSC amplitude) and the number of release site (RRP) leads us to question whether p is developmentally regulated. Figure 3*D* shows that, at P1, p was significantly higher (0.36 ± 0.02, $n = 15$) than at older ages (0.25 ± 0.02, $n = 9$, $P < 0.01$ at P3). No statistically significant difference was observed between the older (from P3 to P22) age groups. The data show that a decrease in release probability contributes to the observed eIPSC amplitude decline between P1 and P3.

However, one should not forget that the calculated release probability values are strongly dependent on the precision of the RRP estimates. RRP underestimation, at P1 for example, could lead to the higher p value. As the RRP estimate precision is difficult to calculate, we tried to check the reliability of the obtained RRP and p value indirectly. Firstly, the obtained RRP and p value allow calculation of the coefficient of variation (CV) of eIPSC amplitudes as $CV = [(1 - p)/(RRP \times p)]^{1/2}$. If the estimates were correct, the predicted CV should strongly correlate with the calculated CV ($CV = \text{s.d.}\ \text{mean}^{-1}$) of recorded eIPSCs. This was indeed the case (Fig. 4*A*).

Secondly, release probability was shown to affect various forms of short-term plasticity including the paired-pulse ratio (PPR; Thomson, 2000; Zucker & Regehr, 2002), which is independent of the number of release sites. In general, high release probability is reported to be associated with paired-pulse depression, while low p value is associated with paired-pulse facilitation. If the obtained p values were correct, PPR should exhibit an increase at P3. Indeed, strong paired-pulse depression was observed at P1 (PPR, 0.68 ± 0.05, $n = 15$), whereas more mature synapses (starting from P3) exhibited, on average, no paired-pulse modulation (1.03 ± 0.08 at P3, $n = 8$, $P < 0.01$, Fig. 4*B*). However, although PPR is thought to mainly reflect presynaptic properties, it can also be influenced by the state of postsynaptic receptors (Kirischuk *et al.* 2002). To estimate the latter contribution, we investigated the correlation between eIPSC kinetics and PPR. No correlation was found at any age tested (minimal

$P > 0.25$, Fig. 4*C*) thereby minimizing the possibility that the observed increase in PPR was associated with the shortening of eIPSCs. Moreover, PPR inversely correlated with p at all ages tested, i.e. independent of eIPSC duration (Fig. 4*D*). This indicates that paired-pulse depression has a presynaptic origin in the present preparation.

Therefore we conclude that the calculated p values are reliable, and accept that p experiences a significant drop shortly after birth.

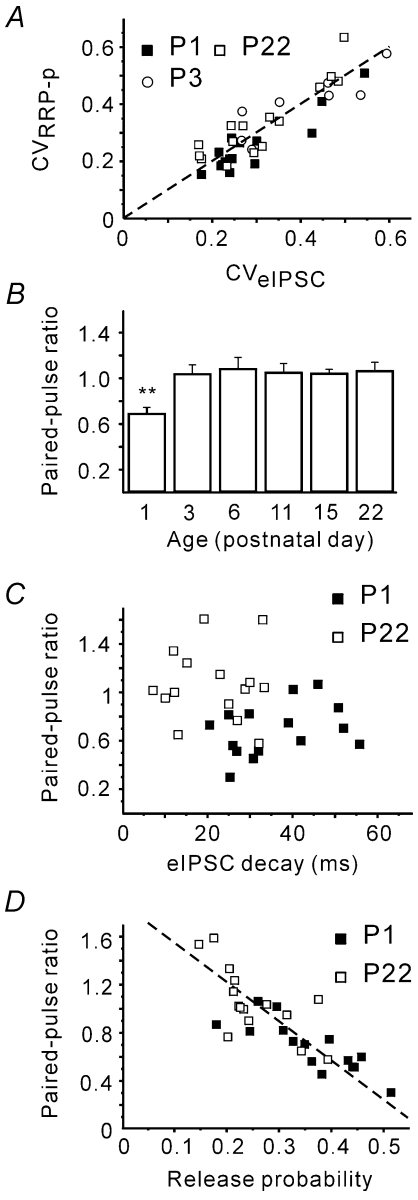

Figure 4. Calculated RRP and *p* estimates are reliable
A, eIPSC coefficient of variation (CV) was calculated using either recorded eIPSCs (CV = S.D. mean^{-1}) or obtained RRP and p values (CV = $((1-p)/(\mathrm{RRP}\times p))^{1/2}$. The dashed line corresponds to a 1 : 1 ratio. *B*, changes in the paired-pulse ratio (PPR, $\mathrm{eIPSC}_2/\mathrm{eIPSC}_1$) early during postnatal development. PPR at P1 was significantly smaller. *C*, there was no correlation between PPR and eIPSC decay kinetics. *D*, PPR and calculated release probabilities negatively correlated at all ages tested (only P1 and P22 shown).

Tetanic depression of eIPSC amplitudes

During high frequency stimulation, higher release probability should result in a stronger eIPSC depression as a consequence of presynaptic vesicle depletion. Therefore, we analysed whether the depression of eIPSC amplitudes during 50-Hz trains (tetanic depression) is dependent on age. The insets of Fig. 5*A* show that the steady-state release patterns differ at P1 and P22. Amplitudes of stimulus-locked eIPSCs (i.e. the IPSCs occurring within a 3-ms interval after a stimulus; see Methods), appeared to be smaller at P1 than at P22. To make the eIPSCs recorded from different cells comparable, eIPSC amplitudes were normalized to q and RRP. Figure 5*B* shows that the steady-state eIPSC amplitude, i.e. the mean eIPSC amplitude in response to the last 10 pulses, was significantly larger at P22 than at P1 (0.14 ± 0.01 and 0.07 ± 0.01, $n = 15$, $P < 0.01$). The steady-state

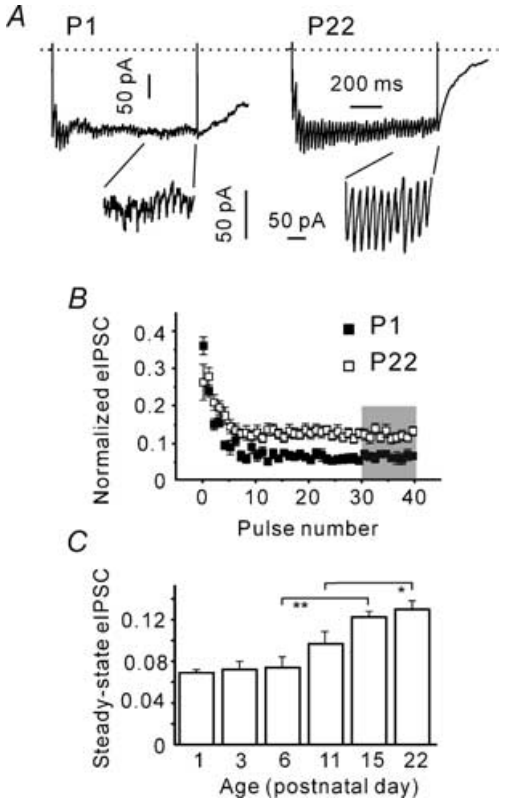

Figure 5. Reduction in tetanic eIPSC depression during development
A, sample traces representing compound IPSCs induced by trains of 40 pulses at 50 Hz. Insets show that the synchronous component (stimulus-locked eIPSCs) during the late phase of stimulation are larger at P22 as compared to P1. *B*, dependence of stimulus-locked eIPSC amplitudes on the pulse number. Measured amplitudes were normalized to the RRP size and q. Averaged data from 15 cells in each age group. *C*, statistical data from all age groups. The last 10 eIPSCs (shaded area in *B*) in the trains were averaged and normalized to q and RRP. Note an increase in the steady-state eIPSC amplitude during development.

eIPSC amplitudes displayed a significant increase during development and main changes occurred between P6 and P15 (Fig. 5*C*). The steady state eIPSC amplitudes were 0.73 ± 0.02, 0.87 ± 0.03 and 0.11 ± 0.01 at P6 ($n = 9$), P11 ($n = 8$) and P15 ($n = 9$), respectively. We conclude that the tetanic depression gets weaker during postnatal development.

The steady-state release rate at individual release sites is not age-dependent

However, high frequency stimulation is known to lead to a significant increase in the presynaptic Ca^{2+} concentration.

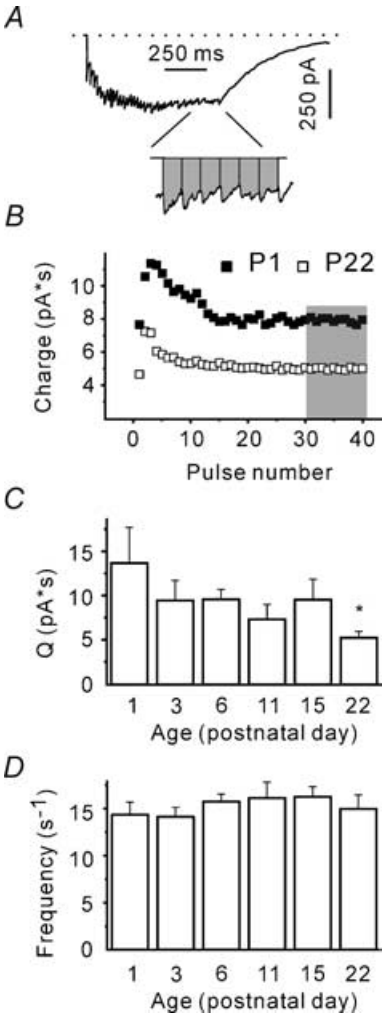

Figure 6. The steady-state release rate at single release site is not dependent on age

A, sample trace representing a compound IPSC in response to a train of 40 pulses at 50 Hz. Trace is an average of 10 responses. Integral under the current curve represents the charge (inset). *B*, interstimulus charge transfer reaches steady state after 20 pulses. Data from individual cells at P1 and P22. *C*, steady-state charge calculated as mean interstimulus charge transfer (Q) over the last 10 pulses (shaded area in *B*) decreases during development. *D*, plot showing the steady-state release rates at single release sites at different ages. Steady-state release rate was calculated as $F = Q/(\mathrm{ISI} \times \mathrm{RRP} \times \mathrm{dIPSC}_{\mathrm{change}})$.

The latter can intensify not only the stimulus-locked release, but also asynchronous release (Lu & Trussell, 2000; Kirischuk & Grantyn, 2003). Therefore we examined whether total (synchronous plus asynchronous) release display age dependence. In this case, interstimulus charge transfer was taken as a measure of release (Fig. 6*A*). The interstimulus charge transfer reached a plateau after 10–20 pulses (Fig. 6*B*). Therefore, the steady-state charge was defined as the mean interstimulus charge transfer (Q) over the last 10 pulses. It was found that Q was significantly smaller at P22, as compared to the other age groups ($P < 0.05$, Fig. 6*C*). Under steady state conditions, Q represents the total release and is proportional to the quantal charge (q_c), the number of release sites (N), the mean frequency of vesicle liberation at a single release site (F), and interstimulus interval (ISI): $Q = q_c NF \times \mathrm{ISI}$. Estimates for the first two parameters (q_{dIPSC} and RRP, respectively) are available. Therefore, the steady-state frequency of vesicle liberation at a single release site can be calculated. It amounts to about $15\ \mathrm{s}^{-1}$ and lacks an age dependence (minimal $P > 0.25$, Fig. 6*D*). We conclude that after RRP depletion, individual release sites liberate vesicles at similar frequencies at all ages investigated; that is, the total release appeared to be age independent.

Developmental increase in release synchrony

As the total release is age-independent, a developmental reduction of the tetanic eIPSC depression (Fig. 5*C*) suggests that more mature terminals release more vesicles synchronously even after RRP depletion. However, this conclusion is strongly dependent on the precision of RRP, q and q_c estimates. Therefore, to not be dependent on the estimates, we tried to verify this hypothesis by calculating the charge transfers mediated by synchronous and asynchronous release (Kirischuk & Grantyn, 2003). To do this, a train-induced eIPSC response was composed (see Methods). Stimulus-locked IPSCs were assumed to decay monoexponentially with a time constant equal to that of pretetanic eIPSCs. The compound evoked IPSC was modelled and integrated to obtain the synchronous charge transfer per stimulus (Fig. 7*A*). The difference between the observed and the calculated current integrals represents the charge transfer mediated via asynchronous vesicle release. A synchrony index was defined as the ratio of synchronous to asynchronous charge transfers and was calculated over the last 10 pulses. Figure 7*B* shows that the synchrony index increases during postnatal development, the main changes were observed between P6 and P15. The synchrony indices were 0.31 ± 0.03, 0.39 ± 0.03 and 0.48 ± 0.03 at P6 ($n = 9$), P11 ($n = 8$) and P15 ($n = 9$), respectively, and differed significantly ($P < 0.05$). The data confirm the hypothesis that the balance between synchronous and asynchronous release changes during development.

Delayed release shortens with postnatal development

What could possibly underlie the observed increase in the release synchrony? As GABA release is driven by the presynaptic Ca^{2+} concentration, developmental changes in presynaptic Ca^{2+} signalling may affect the balance between the two release modes. Unfortunately, direct measurements of presynaptic Ca^{2+} concentration were technically difficult to perform in this preparation. Therefore, we studied the developmental changes in the delayed release (DR) that is also driven by presynaptic Ca^{2+} (del Castillo & Katz, 1954; Kirischuk & Grantyn, 2003). Two approaches were used to quantify the DR. First, the decay phase of the averaged responses was fitted with a single exponential function and normalized to the dIPSC decay time. Second, we assumed that in the absence of DR the train-induced response would decay mono-exponentially with a time constant equal to the dIPSC decay time constant, and the area of this hypothetical response was calculated. Next, the area under the current trace was measured over the first 3 s after the termination of stimulation. The difference (Fig. 8*A* and *B*, shaded areas) was normalized to the product of the dIPSC area and the RRP size and was taken as a measure of DR.

We also considered the possibility that 40 stimuli were not sufficient to fully desynchronize the release at more mature synapses, which then could lead to an overestimation of release synchrony. To investigate this possibility, the DR was induced by trains of variable duration (two to 80 pulses). Figure 8*A–C* shows that the DR decreased with age. However, when delayed responses were normalized to the maximal DR induced by a train of 80 pulses, the dependence on the number of pulses was similar at all ages tested. Figure 8*D* represents the curves obtained at P1 and P22. This result suggests that a train of 40 pulses elicits a fully developed DR independently of age.

Next, the developmental changes of delayed response were investigated using trains of 40 pulses. Figure 8*E* and *F* shows that the DR gradually decreased with age. The normalized DR areas were 3.7 ± 0.2, 2.8 ± 0.2 and 1.9 ± 0.3 at P6 ($n = 9$), P11 ($n = 8$) and P15 ($n = 9$), respectively. These values were significantly different from each other ($P < 0.05$). At P15–22, the DR decay time was only about two times longer than the eIPSC decay (40–50 ms, Fig. 8*F*). Given that the DR decay reflects the dynamics of presynaptic Ca^{2+} transients, these results suggest that presynaptic Ca^{2+} buffering/extrusion is becoming more efficient with age, which may underlie the observed increase in release synchrony.

Discussion

In this study we provide detailed information on the developmental changes in the properties of GABAergic synapses. The experiments showed that GABAergic synapses pass through two periods of major changes during postnatal development of the SC. (i) During the first 2–3 days after birth, and coincidental with the onset of glutamatergic spontaneous activity and the switch from depolarizing to hyperpolarizing GABA action (Grantyn *et al.* 2004), the mean release probability decreases. (ii) Before and during the period of eye opening (P6–P15), and coincidental with the shortening of IPSCs due to a subunit exchange (Grantyn *et al.* 2004; Henneberger *et al.* 2005), asynchronous release is down-regulated in favour of stimulus-locked synchronous release.

Changes in the probability of release between P1 and P3

Our data show that the release probability is higher at initial stages of GABAergic synapse development. A developmental reduction in release probability was also reported for other synapses that use glutamate as a neurotransmitter (Bolshakov & Siegelbaum, 1995; Taschenberger & von Gersdorff, 2000; Iwasaki & Takahashi, 2001; Chavis & Westbrook, 2001). However, modification of this important parameter was usually observed during the second/third week of postnatal development. To our surprise, in the inhibitory synapses of the mouse SC the reduction of release probability was observed as early as P3. At this age, in the SC (Grantyn *et al.* 2004) as well as in many other regions of the immature

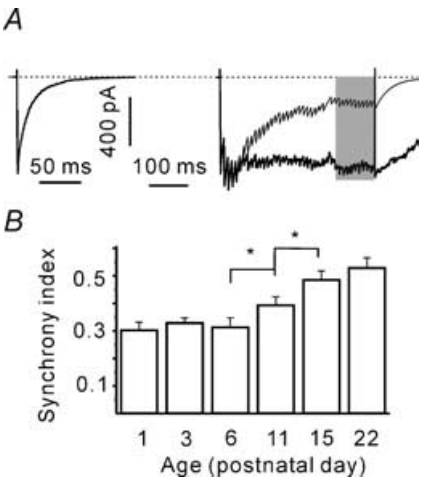

Figure 7. Age-dependent increase of synchronous release during the steady-state phase
A, calculation of synchronous charge transfer. eIPSCs during trains were supposed to decay monoexponentially. Average single eIPSC used to calculate the decay time constant of stimulus-locked events (left). Individual eIPSC amplitudes were measured (see Figure 1*D*). Train-induced eIPSC was modelled (right, thin line) and integrated giving a synchronous charge transfer during the train. The difference between measured and calculated eIPSC charges provides an estimate of asynchronous charge transfer. *B*, the synchrony index increases with age. The synchrony index was defined as the ratio of synchronous to asynchronous charge transfer and was calculated over the last 10 pulses (shaded area in *A*).

CNS (for review see Davies *et al.* 1998; Ben-Ari, 2002), $GABA_A$ receptor activation causes depolarization of the postsynaptic cells mainly because of a low activity level of the chloride extruder KCC2 (Rivera *et al.* 2004).

The present estimate of *p* relies on the correct estimation of RRP size. The latter relies on two assumptions: (i) the number of activated connections remains constant during the stimulus trains; and (ii) the vast majority of vesicles are released synchronously during the steady-state phase. However, at P1 a depolarizing action of GABA may have elicited recurrent activity and recruited additional GABAergic inputs which were not directly activated by electrical stimulation. The latter can increase the slope of the cumulative eIPSC histogram (Fig. 1*E*) and lead to an underestimation of RRP size and, consequently, to an overestimation of release probability. On the other hand, the higher level of asynchronous release at younger ages (Figs 7 and 8) can decrease the slope of the cumulative eIPSC histogram and lead to an overestimation of RRP and to an underestimation of *p*.

There is no direct evidence that would allow us to reject these possibilities. However, our data provide some hints arguing against their significant impact on the RRP estimate. Firstly, if the contribution of the recurrent activity was significant, approaching the steady state would be expected to take longer at P1 than at an older age, when GABA is an inhibitory neurotransmitter. The data show that, independently of age, postsynaptic charge reached the steady state after 10–20 pulses and did not display a further increase during the last half of the stimulation period (Fig. 6*B*). Secondly, the observed coefficient of variation (CV) of eIPSC amplitudes strongly correlated with the CV calculated using the obtained RRP and *p* values at all ages tested (Fig. 4*A*). Thirdly, the paired-pulse ratio, a widely used index for release probability (Katz & Miledi, 1968), also exhibited a strong increase by P3 (Fig. 4*B*). We therefore conclude that the release probability was indeed higher at P1 and approached its new lower level by P3.

A higher release probability at P1 may have important consequences for the activity-dependent modulation of neuronal growth and synaptogenesis. Considering that the number of excitatory synapses in the immature SC is small and most of them are GABAergic (Meier *et al.* 2003), the previsual network activity, like the giant depolarizing potentials (Ben-Ari, 2001), will largely depend on the high release efficacy of GABAergic terminals.

Developmental down-regulation of asynchronous release in favour of stimulus-locked eIPSCs

It is surprising that no significant change in either release probability or paired-pulse ratio was observed during the second critical period around the onset of patterned vision. At this stage, the main observed change on the presynaptic

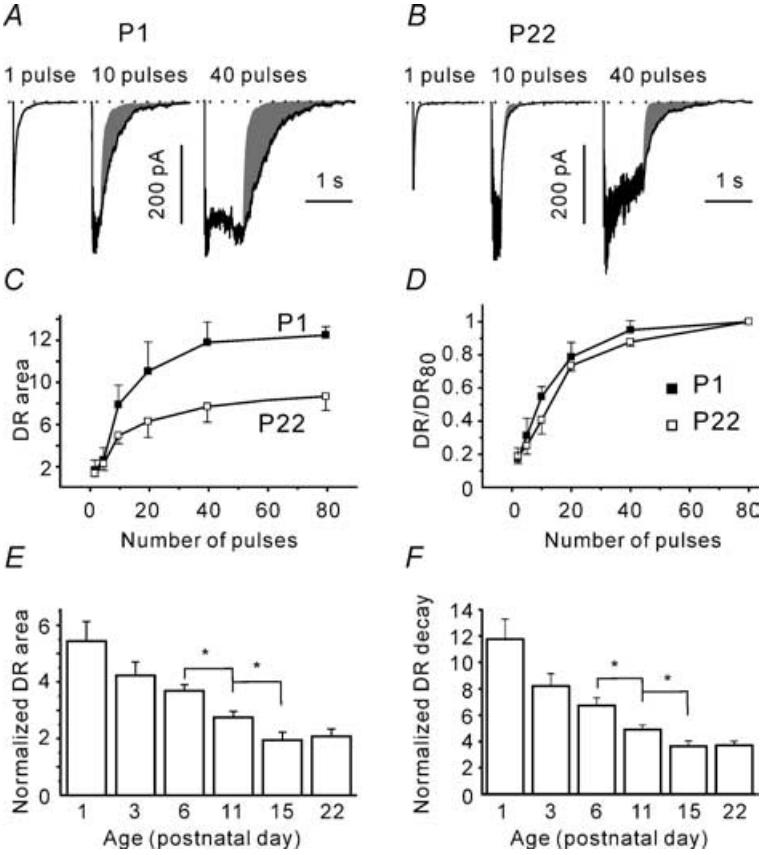

Figure 8. Developmental reduction in delayed release
A and *B*, postsynaptic responses elicited with a single pulse and with trains of 10 and 40 pulses at P1 (*A*) and P22 (*B*). Shaded area represents the delayed response. *C*, dependence of normalized charge transferred after the termination of stimulation on the number of pulses in a train. The delayed response was normalized to the mean charge of the dIPSCs and the RRP size ($n = 5$–15). *D*, at different ages (P1 and P22 shown), the delayed responses exhibit a similar dependence on the train duration. For each cell, the DR values were normalized to the DR response elicited with an 80 pulses train. Same data set as in *C*. *E*, DR declined during development. For each cell, the delayed release area was normalized to the dIPSC area and the RRP. *F*, DR decays faster at older age. The decay of the asynchronous release was fitted by a single exponential function. For each cell, the obtained time constant was normalized to the mean dIPSC decay time constant.

side was the increase in the release synchrony of newly recruited vesicles. A developmental synchronization of the release was already reported for the calyx of Held (Chuhma *et al.* 2001). In this case, the maturation of synapses was accompanied by a shortening of presynaptic Ca^{2+} transients due to an increased endogenous Ca^{2+} binding capacity and Ca^{2+} extrusion rate. Our data are in line with this observation. Although in our preparation we were not able to measure the presynaptic Ca^{2+} concentration directly, the observed drastic shortening of the delayed release (Fig. 8*E* and *F*) is consistent with the hypothesis that presynaptic Ca^{2+} transients become shorter with age. Consequently, the steady-state bulk Ca^{2+} concentration during long trains may be much smaller in more mature synapses decreasing the chances for asynchronous vesicle release.

However an alternative explanation may be that the developmental maturation of presynaptic terminals results in the generation and/or the increase in the number of vesicles with low release probability. At the calyx of Held, newly recruited vesicles were shown to exhibit lower release probability than the RRP vesicles (Wu & Borst, 1999). Sakaba & Neher (2001) extended the above observation and suggested that the RRP contains two populations of vesicles: (i) rapidly releasable (high probability) vesicles with a slow recycling kinetics; and (ii) slowly releasable (low probability) vesicles with a much higher recycling rate. The existence of several populations of presynaptic vesicles at collicular synapses is difficult to prove directly. However, if the fraction of low release probability vesicles in the RRP increased during development, the fraction of the RRP released in response to a single stimulus, i.e. the release probability, would decrease. In contrast to this suggestion, our data show no significant developmental change in the release probability during the critical time period. Therefore, we conclude that the vesicle fraction with low release probability does not change during development.

It is worth mentioning that the dependence of the delayed release on the number of pulses was age independent (Fig. 8*D*). In addition, the total release (postsynaptic charge transfer) reached a steady state after about 20 pulses (Fig. 6*B*) suggesting that the presynaptic Ca^{2+} concentration reaches a steady state after about 20 pulses. As Ca^{2+} buffering/extrusion seems to be faster in more mature synaptic terminals, one can suggest that the steady-state presynaptic Ca^{2+} level is lower at older ages, and this could result in a slower vesicle recycling rate, as vesicle recruitment was shown to be facilitated by an elevated presynaptic Ca^{2+} concentration (Wang & Kaczmarek, 1998; Dittman & Regehr, 1998). Surprisingly, the vesicle release rate during the steady state was similar at all ages tested (Fig. 6*D*). This indicates that the bulk presynaptic Ca^{2+} concentration is high enough to fully accelerate replenishment of the RRP at all ages. At the same time, a stronger presynaptic Ca^{2+} buffering/extrusion can result in a substantial decrease in both size and life time of presynaptic Ca^{2+} microdomains (Llinas *et al.* 1992). The latter might underlie the increase in release synchrony (Meinrenken *et al.* 2002).

The shortening of eIPSCs before and during the period of eye opening

It is already well established that in more mature synapses IPSCs decay much faster (Hestrin, 1992; Takahashi *et al.* 1992; Flint *et al.* 1997; Dunning *et al.* 1999; Hutcheon *et al.* 2000; Vicini *et al.* 2001). We have shown that the acceleration of the IPSC decay kinetics in the SC occurs between P6 and P15. In addition, it was found (Fig. 2*D*) that at any age studied the kinetics of the quantal responses (dIPSCs) was similar to that eIPSCs. This result supports the idea that this developmental change has its origin solely on the postsynaptic side. A recent study from our laboratory reported that the time constant of decay is inversely dependent on the ratio of the $GABA_AR$ $\alpha1/\alpha3$ subunit mRNA level, and this subunit switch requires NMDA receptor activity (Henneberger *et al.* 2005). In the superficial layers of the mouse SC, the peak of NMDA receptor activity is reached at P11 (Grantyn *et al.* 2004). The new and, in our opinion, most noteworthy finding is that the postsynaptic shortening of IPSCs coincides with a presynaptic change that causes a synchronization (shortening) of release.

Physiological relevance: from asynchronous to stimulus-locked inhibition

Our data indicate that at individual release sites new GABA quanta replace the spent ones at an average rate of about $15\,s^{-1}$, and this rate is not dependent on age. However, despite a similar release rate, immature synapses provide better conditions for the summation of postsynaptic currents. At the presynaptic site, desynchronization of release can serve to prevent saturation of slowly deactivating postsynaptic receptors. Consequently, GABAergic inhibition at immature synapses is asynchronous rather than stimulus-locked. Its strength reflects the mean presynaptic firing rate rather than the exact spiking pattern of the presynaptic neurones. With increasing maturity, IPSC shortening and increased release synchrony enable GABAergic synapses to communicate information encoded by the spike-firing pattern of the presynaptic cell. As the SC serves as a novelty detector and guides rapid orienting movements to biologically relevant targets, it should be important that stimulus-locked GABAergic inhibition can persist even after RRP depletion.

References

Ben-Ari Y (2001). Developing networks play a similar melody. *Trends Neurosci* **24**, 353–360.

Ben-Ari Y (2002). Excitatory actions of GABA during development: the nature of the nurture. *Nat Rev Neurosci* **3**, 728–739.

Bolshakov VY & Siegelbaum SA (1995). Regulation of hippocampal transmitter release during development and long-term potentiation. *Science* **269**, 1730–1734.

Brenowitz S & Trussell LO (2001). Maturation of synaptic transmission at end-bulb synapses of the cochlear nucleus. *J Neurosci* **21**, 9487–9498.

Chavis P & Westbrook G (2001). Integrins mediate functional pre- and postsynaptic maturation at a hippocampal synapse. *Nature* **411**, 317–321.

Chuhma N, Koyano K & Ohmori H (2001). Synchronisation of neurotransmitter release during postnatal development in a calyceal presynaptic terminal of rat. *J Physiol* **530**, 93–104.

Davies P, Anderton B, Kirsch J, Konnerth A, Nitsch R & Sheetz M (1998). First one in, last one out: the role of GABAergic transmission in generation and degeneration. *Prog Neurobiol* **55**, 651–658.

del Castillo J & Katz B (1954). Statistical factors involved in neuromuscular facilitation and depression. *J Physiol* **124**, 574–585.

Dittman JS & Regehr WG (1998). Calcium dependence and recovery kinetics of presynaptic depression at the climbing fiber to Purkinje cell synapse. *J Neurosci* **18**, 6147–6162.

Dunning DD, Hoover CL, Soltesz I, Smith MA & O'Dowd DK (1999). $GABA_A$ receptor-mediated miniature postsynaptic currents and alpha-subunit expression in developing cortical neurons. *J Neurophysiol* **82**, 3286–3297.

Flint AC, Maisch US, Weishaupt JH, Kriegstein AR & Monyer H (1997). NR2A subunit expression shortens NMDA receptor synaptic currents in developing neocortex. *J Neurosci* **17**, 2469–2476.

Fritschy JM, Paysan J, Enna A & Mohler H (1994). Switch in the expression of rat $GABA_A$-receptor subtypes during postnatal development: an immunohistochemical study. *J Neurosci* **14**, 5302–5324.

Grantyn R, Juttner R & Meier J (2004). Development and use-dependent modification of synaptic connections in the visual layers of the rodent superior colliculus. In *The Superior Colliculus*, ed. Hall WC & Moschovakis A, pp. 173–210. CRC Press, London.

Gubellini P, Ben-Ari Y & Gaiarsa JL (2001). Activity- and age-dependent GABAergic synaptic plasticity in the developing rat hippocampus. *Eur J Neurosci* **14**, 1937–1946.

Henneberger C, Juttner R, Schmidt SA, Walter J, Meier J, Rothe T & Grantyn R (2005). GluR- and TrkB-mediated maturation of $GABA_A$ receptor function during the period of eye opening. *Eur J Neurosci* **21**, 431–440.

Hestrin S (1992). Developmental regulation of NMDA receptor-mediated synaptic currents at a central synapse. *Nature* **357**, 686–689.

Holt CE & Harris WA (1998). Target selection: invasion, mapping and cell choice. *Curr Opin Neurobiol* **8**, 98–105.

Hutcheon B, Morley P & Poulter MO (2000). Developmental change in $GABA_A$ receptor desensitization kinetics and its role in synapse function in rat cortical neurons. *J Physiol* **522**, 3–17.

Iwasaki S, Momiyama A, Uchitel OD & Takahashi T (2000). Developmental changes in calcium channel types mediating central synaptic transmission. *J Neurosci* **20**, 59–65.

Iwasaki S & Takahashi T (2001). Developmental regulation of transmitter release at the calyx of Held in rat auditory brainstem. *J Physiol* **534**, 861–871.

Jones MV & Westbrook GL (1995). Desensitized states prolong $GABA_A$ channel responses to brief agonist pulses. *Neuron* **15**, 181–191.

Juttner R, Meier J & Grantyn R (2001). Slow IPSC kinetics, low levels of alpha1 subunit expression and paired-pulse depression are distinct properties of neonatal inhibitory GABAergic synaptic connections in the mouse superior colliculus. *Eur J Neurosci* **13**, 2088–2098.

Katz B & Miledi R (1968). The role of calcium in neromuscular facilitation. *J Physiol* **195**, 481–492.

Kirischuk S, Clements JD & Grantyn R (2002). Presynaptic and postsynaptic mechanisms underlie paired pulse depression at single GABAergic boutons in rat collicular cultures. *J Physiol* **543**, 99–116.

Kirischuk S & Grantyn R (2003). Intraterminal Ca^{2+} concentration and asynchronous release at single GABAergic boutons in rat collicular cultures. *J Physiol* **548**, 753–764.

Llinas R, Sugimori M & Silver RB (1992). Microdomains of high calcium concentration in a presynaptic terminal. *Science* **256**, 677–679.

Lu T & Trussell LO (2000). Inhibitory transmission mediated by asynchronous transmitter release. *Neuron* **26**, 683–694.

Meier J, Akyeli J, Kirischuk S & Grantyn R (2003). $GABA_A$ receptor activity and PKC control inhibitory synaptogenesis in CNS tissue slices. *Mol Cell Neurosci* **23**, 600–613.

Meinrenken CJ, Borst JG & Sakmann B (2002). Calcium secretion coupling at calyx of held governed by nonuniform channel-vesicle topography. *J Neurosci* **22**, 1648–1667.

Mishina M, Takai T, Imoto K, Noda M, Takahashi T, Numa S, Methfessel C & Sakmann B (1986). Molecular distinction between fetal and adult forms of muscle acetylcholine receptor. *Nature* **321**, 406–411.

Mize RR (1996). Neurochemical microcircuitry underlying visual and oculomotor function in the cat superior colliculus. *Prog Brain Res* **112**, 35–55.

Mori-Kawakami F, Kobayashi K & Takahashi T (2003). Developmental decrease in synaptic facilitation at the mouse hippocampal mossy fibre synapse. *J Physiol* **553**, 37–48.

Okada M, Onodera K, Van Renterghem C, Sieghart W & Takahashi T (2000). Functional correlation of $GABA_A$ receptor alpha subunits expression with the properties of IPSCs in the developing thalamus. *J Neurosci* **20**, 2202–2208.

Pouzat C & Hestrin S (1997). Developmental regulation of basket/stellate cell – >Purkinje cell synapses in the cerebellum. *J Neurosci* **17**, 9104–9112.

Rivera C, Voipio J, Thomas-Crusells J, Li H, Emri Z, Sipila S, Payne JA, Minichiello L, Saarma M & Kaila K (2004). Mechanism of activity-dependent downregulation of the neuron-specific K-Cl cotransporter KCC2. *J Neurosci* **24**, 4683–4691.

Sakaba T & Neher E (2001). Calmodulin mediates rapid recruitment of fast-releasing synaptic vesicles at a calyx-type synapse. *Neuron* **32**, 1119–1131.

Schneggenburger R, Meyer AC & Neher E (1999). Released fraction and total size of a pool of immediately available transmitter quanta at a calyx synapse. *Neuron* **23**, 399–409.

Takahashi T, Momiyama A, Hirai K, Hishinuma F & Akagi H (1992). Functional correlation of fetal and adult forms of glycine receptors with developmental changes in inhibitory synaptic receptor channels. *Neuron* **9**, 1155–1161.

Taschenberger H & von Gersdorff H (2000). Fine-tuning an auditory synapse for speed and fidelity: developmental changes in presynaptic waveform, EPSC kinetics, and synaptic plasticity. *J Neurosci* **20**, 9162–9173.

Thomson AM (2000). Facilitation, augmentation and potentiation at central synapses. *Trends Neurosci* **23**, 305–312.

Thong IG & Dreher B (1986). The development of the corticotectal pathway in the albino rat. *Brain Res* **390**, 227–238.

Vicini S, Ferguson C, Prybylowski K, Kralic J, Morrow AL & Homanics GE (2001). $GABA_A$ receptor alpha1 subunit deletion prevents developmental changes of inhibitory synaptic currents in cerebellar neurons. *J Neurosci* **21**, 3009–3016.

Wang LY & Kaczmarek LK (1998). High-frequency firing helps replenish the readily releasable pool of synaptic vesicles. *Nature* **394**, 384–388.

Warton SS & McCart R (1989). Synaptogenesis in the stratum griseum superficiale of the rat superior colliculus. *Synapse* **3**, 136–148.

Wu LG & Borst JG (1999). The reduced release probability of releasable vesicles during recovery from short-term synaptic depression. *Neuron* **23**, 821–832.

Zhang LI, Tao HW, Holt CE, Harris WA & Poo M (1998). A critical window for cooperation and competition among developing retinotectal synapses. *Nature* **395**, 37–44.

Zucker RS & Regehr WG (2002). Short-term synaptic plasticity. *Annu Rev Physiol* **64**, 355–405.

Acknowledgements

We would like to express our particular gratitude to Professor R. Baker, New York University Medical Centre, and Dr C. Henneberger, Berlin, Germany for critical reading and helpful comments on an earlier version of the manuscript. The technical assistance of Mrs Kerstin Rückwardt is highly appreciated. This study was supported by the DFG (Deutsche Forschungsgemeinschaft, Project Grant SFB515-B2 to R.G.).